Accepted Manuscript

Title: A Novel Motor Imagery Hybrid Brain Computer
Interface Using EEG and Functional Transcranial Doppler
Ultrasound

Authors: Aya Khalaf, Ervin Sejdic, Murat Akcakaya

Please cite this article as: Khalaf A, Sejdic E, Akcakaya M, A Novel
Motor Imagery Hybrid Brain Computer Interface Using EEG and Functional
Transcranial Doppler Ultrasound, *Journal of Neuroscience Methods* (2018),
https://doi.org/10.1016/j.jneumeth.2018.11.017

A Novel Motor Imagery Hybrid Brain Computer Interface Using EEG and Functional Transcranial Doppler Ultrasound

Aya Khalaf*[1], Ervin Sejdic[1], Murat Akcakaya[1]

Electrical and Computer Engineering Department, University of Pittsburgh, PA, USA. Corresponding author's email: afk17@ pitt.edu.

[1]Electrical and Computer Engineering, University of Pittsburgh, 3700 O'Hara St, Pittsburgh, PA 15213, USA

Highlights

- We introduce a novel hybrid BCI that uses EEG and fTCD as brain sensing modalities.
- Flickering mental rotation and word generation mental tasks were employed.
- Features derived from EEG and fTCD power spectrum were calculated.
- Mutual information and SVM were used for feature selection and classification.
- The proposed hybrid BCI outperforms EEG-fNIRS BCIs in literature in terms of speed.

Abstract— Background: Hybrid brain computer interfaces (BCIs) combining multiple brain imaging modalities have been proposed recently to boost the performance of single modality BCIs. *New method:* In this paper, we propose a novel motor imagery (MI) hybrid BCI that uses electrical brain activity recorded using Electroencephalography (EEG) as well as cerebral blood flow velocity measured using functional transcranial Doppler ultrasound (fTCD). Features derived from the power spectrum for both EEG and fTCD signals were calculated. Mutual information and linear support vector machines (SVM) were employed for feature selection and classification. *Results:* Using the EEG-fTCD combination, average accuracies of 88.33%, 89.48%, and 82.38% were achieved for right arm MI versus baseline, left arm MI versus baseline, and right arm MI versus left arm MI respectively. Compared to performance measures obtained using EEG only, the hybrid system provided significant improvement in terms of accuracy by 4.48%, 5.36%, and 4.76% respectively. In addition, average transmission rates of 4.17, 5.45, and 10.57 bits/min were achieved for right arm MI versus baseline, left arm MI versus baseline, and right arm MI versus left arm MI respectively. *Comparison with existing methods:* Compared to EEG-fNIRS hybrid BCIs in literature, we achieved similar or higher accuracies with shorter task duration. *Conclusions:* The proposed hybrid system is a promising candidate for real-time BCI applications.

Keywords—**Electroencephalogram, Functional Transcranial Doppler Ultrasound, Hybrid Brain Computer Interfaces, Mutual Information, Classification.**

I. INTRODUCTION

B RAIN computer interfaces (BCIs) translate brain activity into control signals that can be used to command external devices such as prosthetic limbs or wheelchairs [1],[2]. The main objective of BCIs is to either bypass or restore neuromuscular activity for individuals experiencing neurological deficits that cause motor impairment such as stroke, Parkinson's disease, and amyotrophic lateral sclerosis [3]. Therefore, developing BCIs is essential for those individuals to communicate with the surrounding environment using only their brain signals. In addition, BCIs have other diverse applications such as control of

humanoid robots [4], and aircrafts [5] as well as controlling virtual reality environments [6].

To design noninvasive BCI systems, different modalities have been investigated including near-infrared spectroscopy (NIRS) [7], functional magnetic resonance imaging (fMRI) [8], and magnetoencephalography (MEG) [9]. However, these modalities have limitations that hamper BCI usage outside controlled laboratory environments. For instance, fMRI and MEG are expensive nonportable equipment that can be used efficiently only in a controlled environment [10]. On the other hand, NIRS does not require highly controlled environment, but it lacks the speed needed for real-time BCIs [11]. Given these limitations of the previously mentioned modalities, most of the existing BCIs use electroencephalograph (EEG) as the input modality since it is portable and cost-effective. Moreover, it has high temporal resolution, therefore, it can be used for developing real-time BCIs.

Among the existing diverse EEG-based BCI categories, BCIs based on motor imagery have been intensively used in rehabilitation applications that seek assisting disabled individuals as well as restoring individual's physical and cognitive functions lost due to neural disorders [12]. Motor imagery (MI) is the process of movement imagination without any actual muscle activation. It was found that the MI process activates the same brain regions activated during the actual physical movement [13]. Therefore, during the rehabilitation process, patients with motor impairments practice MI process to activate the injured brain motor regions [14]. Several studies were performed on both healthy participants and participants with physical and/or speech impairments to examine the feasibility of motor imagery for BCI applications [13], [15], [16]. Towards motor recovery after stroke, several motor imagery BCIs with robotic feedback were developed [14], [17]. Such systems decode the motor imagery signals into robot assisted movements and it was shown that such systems yielded motor improvements.

To boost the performance of MI-based BCI, many studies suggested using NIRS as a second modality to be simultaneously acquired with the EEG [18], [19] since it is less sensitive to electrical noise as well as motion artifacts [20]. However, as mentioned earlier, NIRS is difficult to setup and has a very slow response time [21]. Therefore, to avoid NIRS disadvantages, we suggest Functional transcranial Doppler (fTCD) ultrasound to be simultaneously recorded with EEG for MI-based BCI. Compared to NIRS, fTCD has a faster response time [22]. In addition, it is easier to setup and requires less number of sensors. fTCD assesses the cerebral blood velocity using two ultrasound sensors placed on the left-side and right-side transtemporal window located above the zygomatic arch [23]. It was observed that signals recorded using fTCD change with different cognitive tasks. Based on this observation, a study suggested that it is possible to develop a BCI that is based on fTCD modality using mental rotation and word generation cognitive tasks [24]. However, an observation period of 45 seconds was required to achieve acceptable accuracy which is not practical for a real-time BCI. Towards more efficient fTCD-based BCIs, shorter observation periods (15-20 seconds) were achieved [25], [26]. In a recent study, we examined fTCD as an approach for real-time BCI [27] and achieved approximately 80% accuracy within 5 seconds of the task onset.

It was found that the cerebral blood velocity in left and right middle cerebral arteries (MCAs) changes depending on whether the moving arm is the left or the right one [28]. Such findings suggest that fTCD might be promising for MI-based BCIs. Inspired by these findings as well as the results we achieved previously with fTCD as a candidate for real-time BCIs, we propose MI-based hybrid BCI that uses both EEG and fTCD modalities. Such system will acquire the electrical activity of the brain using the EEG and the vascular response of the brain using the fTCD. We claim that combining these modalities will result in a system with higher performance accuracy, faster response time, and less setup complexity. In this paper, cognitive tasks including left arm MI and right arm MI are considered for the BCI design. Three different binary selection problems were formulated to study the feasibility
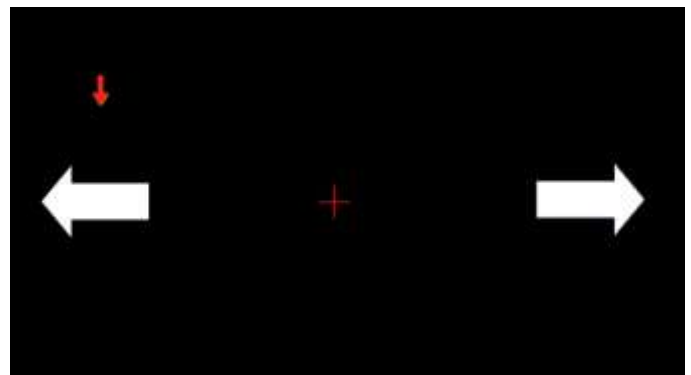
Fig. 1. Stimulus presentation for the hybrid BCI system.

of 2-class BCI. The first two classification problems are formulated to differentiate between each cognitive task and the baseline while the third problem aims at classification of the left arm and right arm MI tasks against each other. For the 3 binary selection problems, features derived from the power spectrum for both EEG and fTCD signals were calculated. In addition, mutual information and linear support vector machines (SVM) were used for feature selection and classification.

II. MATERIALS AND METHODS

A. Simultaneous Data Acquisition

EEG was collected using 16 electrodes placed according to the 10-10 system over frontal, central, and parietal lobes at positions Fp1,Fp2,F3,F4,Fz,Fc1,Fc2,Cz,P1,P2,C1,C2,Cp3, Cp4,P5,and P6. Left mastoid was used as the reference for all participants. A g.tec EEG system with g. USBamp, a bio-signal amplifier, was used in this study. It included 16 24-bit simultaneously sampled channels with an internal digital signal filtering and processing unit and sampling rate up to 38.4 kHz. The data were digitized with a sampling rate of 256 samples/sec and filtered by the amplifier's 8th order bandpass filter with corner frequencies 2, 62 Hz in addition to 4th order notch filters with corner frequencies 58, 62 Hz. Through band-pass filter, our aim was to remove possible DC drift and high frequency noise. Processed data were transferred from the amplifiers to a laptop via USB 2.0.

The fTCD data was collected with two 2 MHz transducers using SONARA TCD system of 145 Mw ultrasonic power. These transducers were placed on the left and right sides of the transtemporal window located above the zygomatic arch. Since the middle cerebral arteries (MCAs) provide approximately 80% of the brain with blood [29], the fTCD depth was set to 50 mm which is the depth of the mid-point of the MCAs [30].

B. Visual Presentation Design

In this presentation scheme, a basic motor imagery task is visualized while acquiring EEG and fTCD simultaneously. As seen in Fig. 1, the screen shows a horizontal arrow pointing to the right representing right arm MI and another horizontal arrow pointing to the left representing left arm MI as well as a fixation cross that represents the baseline. Each trial lasts for 10 s. During each trial, a vertical small arrow, shown in Fig. 1, points randomly to one of the 3 tasks for duration of 10 s and the user has to take rest if the vertical arrow points to the fixation cross or to imagine moving either left or right arm depending on which MI task is specified by the vertical arrow. A total of 150 trials are presented per session.

C. Participants

10 healthy right-handed subjects including 4 males and 6 females participated in the experiment with ages ranging from 23 to 32 years old (mean and standard deviation: 26.7±2.3). The experiment lasted for approximately 1 hour and 15 min including the time required for the setup. All research procedures were approved by local Institutional Review Board (IRB) under the University of Pittsburgh IRB number of PRO16080475. Participants signed a written informed consent before starting the experiment. During the experiment, subjects were seated in a comfortable chair approximately 1 m away from the screen. Each participant attended one session.

D. Feature Extraction and Fusion

The 16-channel EEG data as well as the two-channel fTCD data corresponding to each task were segmented and extracted. For each segment, the power spectrum was estimated using Welch method [31]. The features corresponding to each segment included the raw power spectrum for that segment. The number of features obtained from each power spectrum was reduced by considering the average power over a narrow range of frequencies instead of using all the power spectrum values at all frequency bins as features. The average power over each consecutive 2 Hz for the EEG data was obtained. Since the fTCD signal has much higher bandwidth (≈2.5 KHz) compared to the EEG signals (≈60 Hz), and considering the need to reduce the number of features, the average power over each consecutive 50 Hz for the fTCD data was obtained to form reduced power spectrums. For each observation, EEG feature vector was formed by concatenating reduced power spectrums corresponding to the 16 EEG segments while fTCD feature vector was formed by concatenating reduced power spectrums corresponding to the 2 fTCD segments. For each observation, the overall feature vector was formed by concatenating the EEG feature vector and the fTCD feature vector. The feature vector representing each trial contained 420 features including 320 EEG features as well as 100 fTCD features. Specifically, 20 features were extracted from each EEG electrode giving a total of 320 features whereas each fTCD sensor contributed 50 features giving a total of 100 fTCD features.

E. Feature Selection

Feature selection algorithms are extensively used to improve the prediction accuracy and to reduce computational expenses which is a major issue for real time applications such as BCIs. In this paper, mutual information [32] was used to select the most significant features out of the original feature vector. Mutual information measures how much information can a random variable inform about another variable. In the context of feature selection, mutual information measures the contribution of each feature towards making a correct decision and assigns each feature a score based on that contribution [33]. In other words, the higher the mutual information score is, the higher the contribution of that feature in making a correct classification. The scores were arranged in a descending order. To choose the number of features to be selected, we calculated the cumulative distribution function (CDF) for the scores. CDF thresholds corresponding to the probabilities ranging from 0.5 to 0.95 with a step of 0.05 as well as 0.98 and 0.99 were calculated. The features corresponding to these CDF thresholds were selected. The performance measures (accuracy, sensitivity, and specificity) corresponding to each CDF threshold were calculated.

F. Classification

Support vector machine (SVM) is a supervised machine learning algorithm [34]. Basic SVM is a linear classifier that seeks finding optimal hyper-plane with the largest distance to the closest observation in the training dataset by solving an optimization problem using linear programming. Given that the observations in the feature space are not typically linearly separable, non-linear kernels are usually used to transform observations to a higher dimensional feature space where the classes can be separated linearly. Common kernels include polynomial, and radial basis function (RBF) kernels. However, we used linear SVM in this paper to reduce computational expenses.

To investigate the feasibility of 2-class BCI, three binary classification problems were formulated including right arm MI versus baseline, left arm MI versus baseline, and right arm MI versus left arm MI. Based on the classification results, we calculated some performance measures to evaluate the hybrid system. These measures included accuracy, sensitivity, specificity, and information transfer rate (ITR), known also as the bit rate, given by (1).

$$B = log_2(N) + Plog_2(P) + (1 - P)log_2\left(\frac{1 - P}{N - 1}\right) \qquad (1)$$

where N is the number of classes, P is the classification accuracy and B is the data transmission rate per trial.

G. Evaluation of the Effectiveness of the Hybrid System

The Wilcoxon signed-rank test [35] is a nonparametric hypothesis test used to assess two groups with paired observations. The null hypothesis assumes that the difference between the 2 groups follows a zero-median distribution. The Wilcoxon test returns the p-value for that null hypothesis. To evaluate the significance of the EEG-fTCD combination compared to the system using EEG only, Wilcoxon signed-rank test was used to statistically compare the accuracies and bit rates obtained using the combination to those obtained using EEG only. In particular, EEG-fTCD accuracy vector as well as EEG only accuracy vector containing the accuracies of the 10 participants represented the two groups to be compared. Moreover, same comparison was performed between EEG-fTCD bit rate vector and the bit rate vector obtained using EEG only.

III. RESULTS

Subject-specific classification was performed on each participant using leave-one-out cross validation. For each participant, we analyzed the accuracy profile across time using an incremental window the width of which increases by 1 s. The maximum width for the incremental window is 10 s which represents the trial length. The accuracy analysis was performed using 12 different CDF thresholds corresponding to probabilities ranging from 0.5 to 0.95 with 0.05 step as well as the thresholds corresponding to probabilities of 0.98, and 0.99. Therefore, 12 different accuracy profiles across time were obtained per participant. Average performance measures over all participants were obtained using subject-independent and subject-specific CDF thresholds. For subject-independent threshold, the maximum accuracy at each CDF threshold was obtained for each participant yielding 12 different accuracies for each participant corresponding to the 12 CDF thresholds. For each threshold, the average accuracy over all the 10 participants was obtained. The threshold at which the maximum accuracy was achieved was selected as the general CDF threshold that can be used with all participants. For subject-specific thresholds, the maximum accuracy across all the CDF thresholds for each subject was obtained and considered as the subject's performance accuracy. Therefore, in subject-specific analysis, each subject might have different CDF threshold that corresponds to his/her maximum performance accuracy.

Tables 1 through 3 show the maximum accuracy achieved by each participant and the corresponding time calculated using the EEG-fTCD combination. Corresponding sensitivity and specificity values are reported in detail in Tables A1-A6 in the appendix section of this paper. Here, in the results section, we report only the average sensitivities and specificities. To reveal the significance of the hybrid system, same performance measures were calculated using EEG only and fTCD only with the same time interval at which the EEG-fTCD combination gives the maximum accuracy as seen in Tables 1-3. Transmission rates corresponding to the accuracies and times listed in Tables 1 through 3 were also calculated for each binary problem using EEG data, fTCD data, and

TABLE 1
Maximum accuracy (Acc) and the corresponding time for each subject using hybrid system, EEG only, and fTCD only. These measures were obtained for right arm MI vs baseline problem.

Sub_ID	Subject-independent threshold				Subject- specific threshold			
	Time(s)	Acc_EEG	Acc_fTCD	Acc_Hybrid	Time(s)	Acc_EEG	Acc_fTCD	Acc_Hybrid
1	10	91.67%	57.29%	**93.75%**	10	91.67%	59.38%	**94.79%**
2	10	83.33%	56.26%	83.33%	7	91.67%	61.46%	**92.71%**
3	2	79.17%	45.83%	**84.38%**	7	81.25%	51.04%	**86.46%**
4	9	81.25%	55.21%	**87.50%**	9	81.25%	55.21%	**87.50%**
5	9	87.50%	61.46%	**90.63%**	9	87.50%	61.46%	**90.63%**
6	4	72.92%	56.25%	**82.29%**	7	85.42%	56.25%	**86.46%**
7	6	79.17%	56.25%	**83.33%**	6	80.21%	47.92%	**86.46%**
8	7	80.21%	66.67%	**89.58%**	7	81.25%	69.79%	**91.67%**
9	5	73.96%	61.46%	71.88%	5	71.88%	50.00%	**76.04%**
10	10	86.46%	69.79%	**90.63%**	10	86.46%	69.79%	**90.63%**
Mean	**7.2**	81.56%	58.65%	**85.73%**	**7.7**	83.85%	58.23%	**88.33%**

TABLE 2
Maximum accuracy (Acc) and the corresponding time for each subject using hybrid system, EEG only, and fTCD only. These measures were obtained for left arm MI vs baseline problem.

Sub_ID	Subject-independent threshold				Subject- specific threshold			
	Time(s)	Acc_EEG	Acc_fTCD	Acc_Hybrid	Time(s)	Acc_EEG	Acc_fTCD	Acc_Hybrid
1	10	88.66%	74.23%	**93.81%**	10	87.63%	65.98%	**97.94%**
2	7	93.81%	58.76%	92.78%	7	91.75%	65.98%	**93.81%**
3	8	80.41%	46.39%	**89.69%**	4	81.44%	51.55%	**93.81%**
4	2	73.32%	50.52%	**74.23%**	5	78.35%	61.86%	**81.44%**
5	8	77.32%	43.30%	**80.41%**	9	87.63%	53.61%	87.63%
6	2	85.57%	52.58%	**86.60%**	3	74.23%	53.61%	**86.60%**
7	3	88.66%	54.64%	**90.72%**	3	88.66%	54.64%	**90.72%**
8	9	86.60%	55.67%	**88.66%**	9	85.57%	50.52%	**92.78%**
9	5	74.23%	48.45%	**79.38%**	5	74.23%	48.45%	**79.38%**
10	9	87.63%	55.67%	**88.66%**	6	91.75%	47.42%	90.72%
Mean	**6.3**	83.61%	54.02%	**86.49%**	**6.1**	84.12%	55.36%	**89.48%**

TABLE 3
Maximum accuracy (Acc) and the corresponding time for each subject using hybrid system, EEG only, and fTCD only. These measures were obtained for left arm MI vs right arm MI.

Sub_ID	Subject-independent threshold				Subject- specific threshold			
	Time(s)	Acc_EEG	Acc_fTCD	Acc_Hybrid	Time(s)	Acc_EEG	Acc_fTCD	Acc_Hybrid
1	1	86.67%	44.76%	86.67%	1	82.86%	51.43%	**93.33%**
2	5	75.24%	38.10%	75.24%	5	75.24%	38.10%	75.24%
3	10	73.33%	46.67%	**75.24%**	6	71.43%	69.52%	**81.90%**
4	1	82.86%	45.71%	**83.81%**	2	81.90%	53.33%	**85.71%**
5	1	78.10%	50.48%	**81.90%**	1	78.10%	50.48%	**81.90%**
6	3	85.71%	42.86%	83.81%	3	85.71%	42.86%	83.81%
7	4	75.24%	44.76%	71.43%	4	71.43%	43.81%	**79.05%**
8	7	89.52%	45.71%	**92.38%**	9	96.19%	50.00%	**97.14%**
9	1	70.48%	44.76%	**71.43%**	1	70.48%	44.76%	**71.43%**
10	1	65.71%	62.86%	**68.57%**	2	62.86%	66.67%	**74.29%**
Mean	**3.4**	78.29%	46.67%	**79.05%**	**3.4**	77.62%	51.10%	**82.38%**

EEG-fTCD combination as seen in Fig. 2, 3, and 4. Fig. 5 compares average bit rates obtained using subject-independent and subject-specific thresholds for the 3 binary problems. Tables 4, and 5 list the p-values representing the significance of the EEG-fTCD

hybrid system. These p-values are calculated by statistically comparing the EEG-fTCD accuracy/bit rate vector with the EEG only accuracy/bit rate vector for all the binary selection problems when subject-independent and subject-specific CDF thresholds are

used for feature selection.
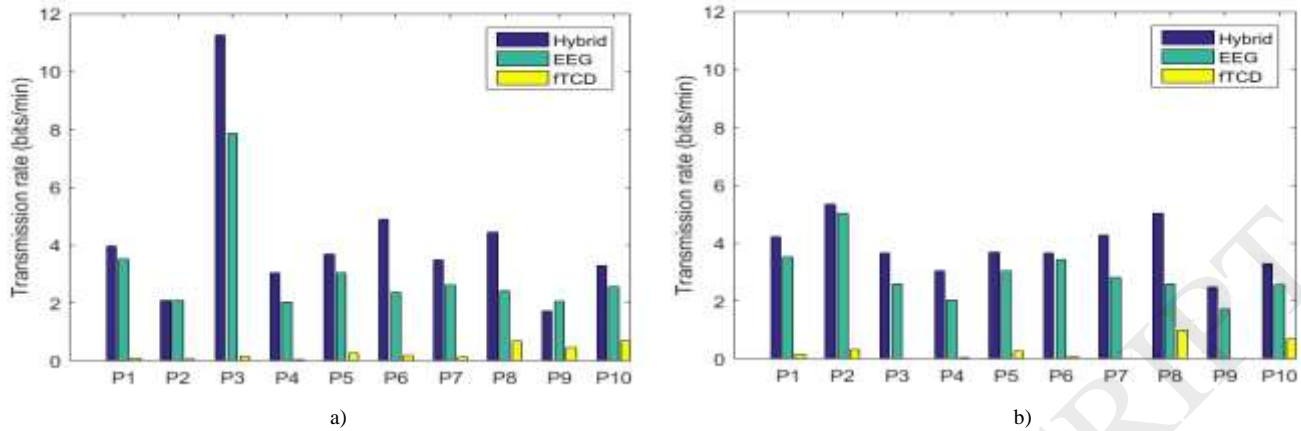
Fig. 2. Transmission rates for each participant (p) calculated using both EEG and fTCD, EEG only, and fTCD only for right arm MI vs baseline problem with a) subject-independent threshold b) subject-specific thresholds.
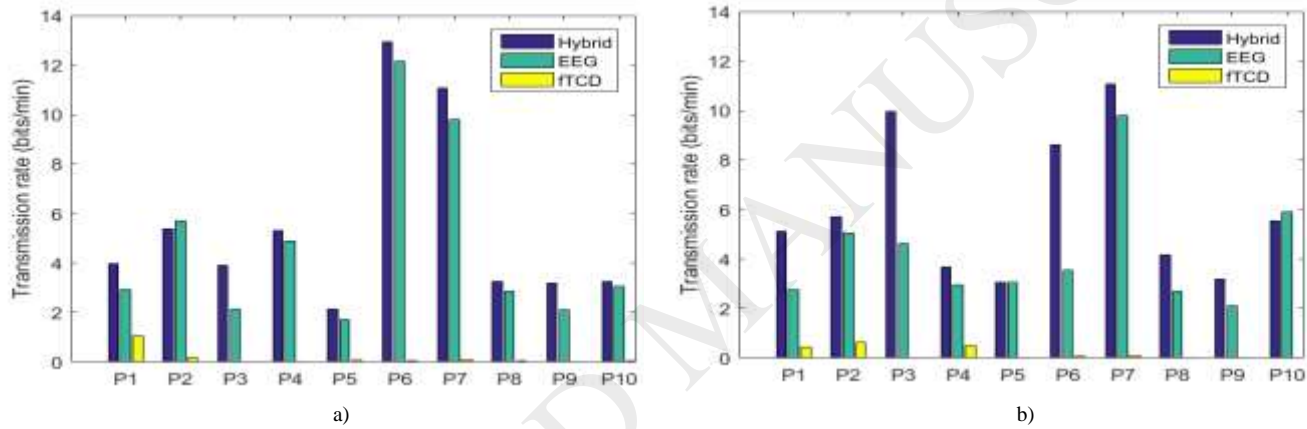
Fig. 3. Transmission rates for each participant (p) calculated using both EEG and fTCD, EEG only, and fTCD only for left arm MI vs baseline problem with a) subject-independent threshold b) subject-specific thresholds.
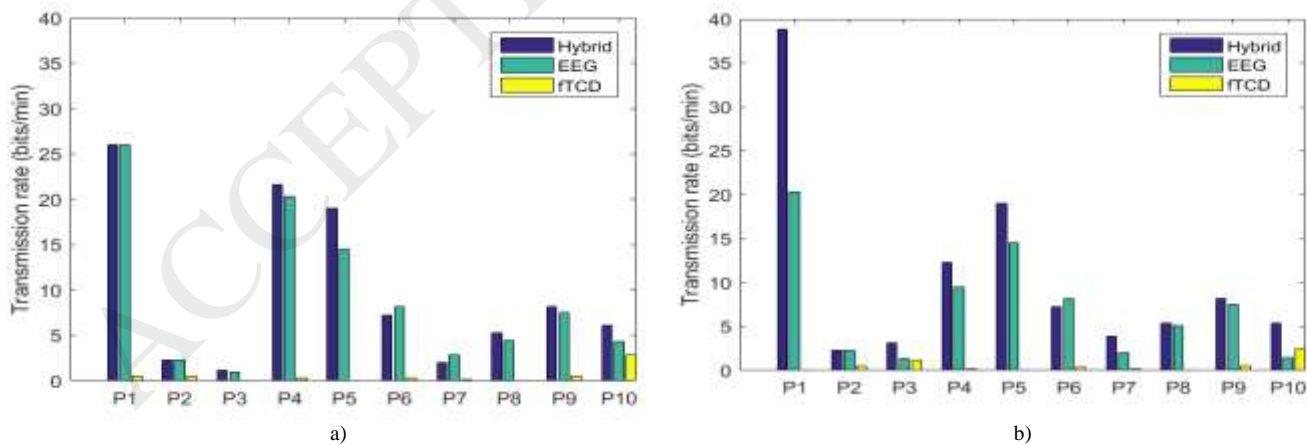
Fig. 4. Transmission rates for each participant (p) calculated using both EEG and fTCD, EEG only, and fTCD only for right arm MI vs left arm MI problem with a) subject-independent threshold b) subject-specific thresholds.

A. *Right/Left arm MI vs Baseline*

Table 1 shows the maximum accuracies and corresponding times for right arm MI versus baseline problem using subject-independent and subject-specific thresholds while appendix Tables A1 through A4 show details about sensitivity and specificity

TABLE 4
P-values representing significance of the EEG-fTCD system in terms of accuracy for the binary problems using subject-independent and subject-specific CDF thresholds.

Threshold	Right MI vs Baseline	Left MI vs Baseline	Right MI vs Left MI
Subject-independent	0.0117	0.0098	0.3828
Subject-specific	0.002	0.0078	0.0195

TABLE 5
P-values representing significance of the EEG-fTCD system in terms of bit rates for the binary problems using subject-independent and subject-specific CDF thresholds.

Threshold	Right MI vs Baseline	Left MI vs Baseline	Right MI vs Left MI
Subject-independent	0.0078	0.0059	0.2500
Subject-specific	0.0020	0.0078	0.0195

values for each individual. For subject-independent threshold analysis, average accuracy, sensitivity and specificity of 85.73%, 87.31%, and 83.86% were achieved using both EEG and fTCD within 7.2 s of the cognitive activity onset. In the meantime, using EEG only, we obtained 81.56%, 85.19%, and 77.27% average accuracy, sensitivity and specificity respectively.

Despite the low fTCD accuracy of 58.65%, when combined with EEG, fTCD data boosted the overall performance of the hybrid system with average accuracy increase of 4.17% compared to the accuracy obtained with the EEG only. As shown in Table 1 and Fig. 2. (a), the EEG-fTCD combination scored higher accuracy and bit rate for 8 out of the 10 participants. In terms of statistical comparison, as seen in Tables 4, and 5 the differences between hybrid and EEG only performance measures were shown to be significant as they correspond to a p-value of 0.012 in terms of accuracy comparison and p-value of 0.0078 in terms of bit rate comparison.

On the other hand, same performance measures were calculated for right arm MI versus baseline problem using subject-specific thresholds as shown in Table 1. It was found that the EEG-fTCD combination achieved 88.33%, 90.96%, and 85.23% average accuracy, sensitivity, and specificity respectively within 7.7s compared to 83.85%. 86.92%, and 80.23% obtained by EEG only and 58.23%, 61.92%, and 53.86% obtained by fTCD only. The average accuracy difference between the hybrid combination and
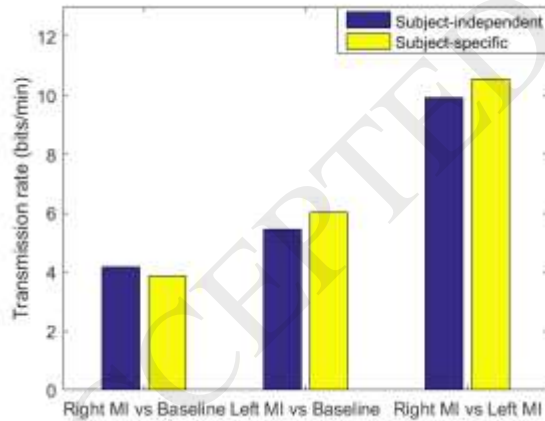
Fig. 5. Average transmission rates calculated using EEG-fTCD combination for the 3 binary problems with subject-independent and subject-specific thresholds.

the EEG only was 4.48%. As seen in Fig. 2. (b), EEG-fTCD combination achieved higher bit rates compared to EEG only for all of the participants using subject-specific thresholds. However, Fig,5 shows that subject-independent threshold obtained slightly higher average transmission rate 4.19 bits/min of compared to 3.87 bits/min for subject-specific threshold. In terms of statistical comparison, the EEG-fTCD combination achieved higher accuracy and bit rate compared to EEG only for all the participants with a p-value of 0.002 for both accuracy and bit rate (Tables 4, and 5).

Table 2 shows the performance measures for left arm MI versus baseline problem using subject-independent and subject-specific thresholds. Using subject-independent threshold, average accuracy, sensitivity and specificity of 86.49%, 87.55%, and 85.23%

were obtained using EEG-fTCD combination within 6.3s. EEG only scored 83.61% accuracy, 85.09% and 81.82% specificity. A difference of 2.89% was achieved with 0.0098 p-value of as seen in Table 4. In terms of bit rates, a p-value of 0.0059 was achieved as shown in Table 5. The hybrid system obtained higher accuracies and bit rates compared to EEG for 9 out of 10 subjects. In contrast, using subject-specific threshold, an average accuracy difference of 5.36% was achieved with a p-value of 0.0078. In terms of bit rates, also, a p-value of 0.0078 was achieved as seen in Table 5. For 8 out of 10 participants, EEG-fTCD scored higher accuracy and bit rate compared to EEG only. EEG-fTCD scored 89.48% accuracy, 91.89% sensitivity, and 86.59% specificity within 6.1s while EEG only scored 84.12% accuracy, 86.42% sensitivity, and 81.36% specificity. Considering Fig. 3, we obtained higher bit rates using EEG-fTCD combination compared to bit rates generated using EEG only and fTCD only. In addition, as seen in Fig. 5, subject-specific thresholds achieved 6.02 bits/min average bit rate compared to 5.45 bits/min for subject-independent threshold.

B.   Right arm MI vs left arm MI
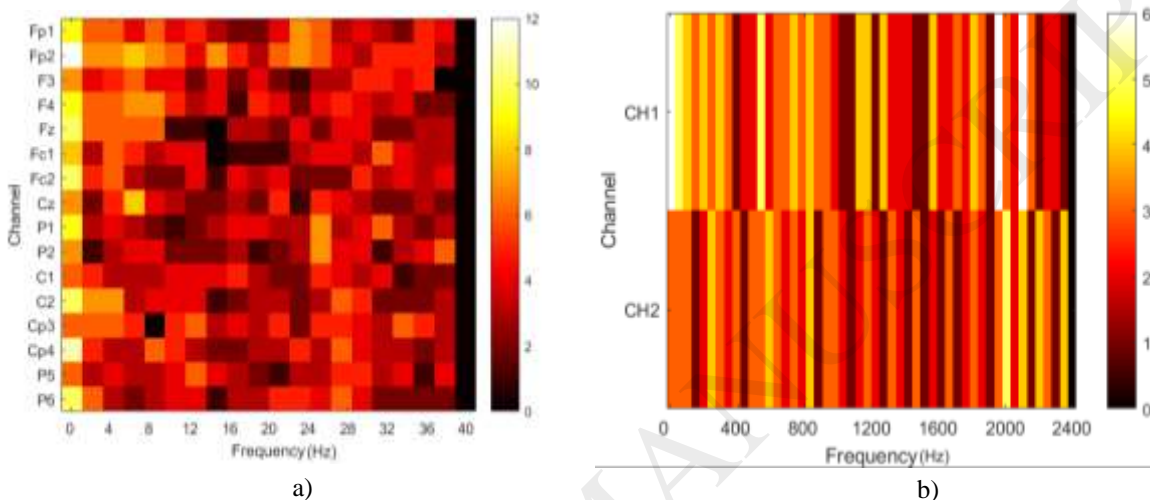
Fig. 6. 2D histogram of the significant features during right arm versus left arm MI at each channel and each frequency window of width 2Hz for EEG and 50 Hz for fTCD. The heat maps demonstrate, across all participants, how many times any of the features within each channel were considered significant. a) EEG histogram for 16 electrodes b) fTCD histogram for right fTCD channel (CH1) and left fTCD channel (CH2).

The maximum accuracies and corresponding times for right arm MI versus left arm MI are shown in Table 3 for subject-independent and subject-specific threshold respectively. See also appendix Tables A5, and A6 for details about sensitivity and specificity values for each individual. Right arm MI versus left arm MI classification achieved 79.05%, 79.04%, and 79.06% average accuracy, sensitivity and specificity respectively using EEG-fTCD combination within 3.4 s while EEG data only obtained average accuracy, sensitivity and specificity of 79.29%, 78.08%, and 78.49% respectively. The average accuracy difference was low and insignificant (p-value=0.3828) according to Table 4. However, subject-specific thresholds obtained higher performance measures as, within 3.4 s, it achieved 82.38% average accuracy, 82.12% sensitivity and 82.64% specificity using the EEG-fTCD combination and 77.62%, 78.65%, and 76.60% using EEG only leading to a significant average accuracy difference of 4.76 % with 0.0195 p-value as seen in Table 4. The EEG-fTCD combination scored higher accuracy for 8 out of 10 participants. On the other hand, bit rates for each participant were calculated and visualized as seen in Fig. 4. It can be noted that the bit rate difference between EEG-fTCD combination and EEG only based on subject-specific threshold is much higher compared to the same difference obtained using subject-independent threshold (p-value of 0.25 compared to p-value of 0.0195). On average, from Fig. 5, 10.57 bits/min and 9.91 bits/min were achieved using subject-specific and subject-independent thresholds respectively.

By Inspecting the selected significant features across all participants for the right arm MI versus left arm MI problem, it was found that, as seen in Fig. 6, across all electrodes, the EEG average power spectrum values at frequencies up to 2 Hz (delta frequency band) are the most common selected features across participants. Moreover, it was found that the common selected features belonging to theta (5-8 Hz) and mu (8–13 Hz) bands are coming from electrodes Fp1, Fp2, F3, and F4 while the common features belonging to beta (16–28 Hz) band are associated with electrodes C1, C2, Cp3, Cp4, P5, and P6. As for the fTCD, the common significant features were found at frequency bands 550-600, 2000-2050 and 2150-2200 Hz for the right fTCD channel and at frequency band 2050-2100 Hz for the left fTCD channel.

IV.   DISSCUSSION

Considering the performance measures reported for the 3 binary classification problems we studied, it is noted that subject-specific thresholds achieved higher performance measures compared to subject-independent threshold. However, the EEG-fTCD combination for right/left MI versus baseline problems was proven to be significant compared to EEG only using also subject-

independent thresholds as seen in Tables 4, and 5. Thus, it is possible to use subject-independent thresholds for right/left MI versus baseline problems. In this case, same analysis can be performed for all participants and no parameter selection (CDF threshold) needs to be performed for each participant. In contrast, the EEG-fTCD combination was shown to be significant for right arm MI versus left arm MI problem using only subject-specific thresholds. Thus, CDF threshold has to be optimized for each participant separately. In terms of accuracy, right/left arm MI versus baseline problems achieved higher accuracy compared to right arm MI versus left arm MI. In contrast, it took approximately 7s on average for right/left MI versus baseline problems to achieve maximum accuracy while right arm MI versus left arm MI problem obtained maximum accuracy within approximately 3 s. Consequently, right arm MI versus left arm MI achieved the highest transmission rate of 10.57 bits/min.

Despite the high accuracies obtained in a previous study with the fTCD data only [27], in this paper, we obtained low accuracy with fTCD data only due to several reasons. It is well known that fTCD can differentiate imagery and analytical tasks since analytical tasks induce higher blood velocity in left MCAs while imagery tasks induce bilateral activation. However, in this paper, both tasks are imagery tasks which makes the classification problem harder to solve. In addition, in the previous study, a 15-min baseline period was recorded before starting the tasks to stabilize the cerebral blood flow. Moreover, a resting period of 45 s was inserted between consecutive tasks. In this paper, no baseline/rest periods were added to stabilize the cerebral blood flow since such periods will reduce the communication speed. In fact, the baseline was shown at random times since it was designed as a task that resembles the condition in which the BCI user does not intend to produce a command. Moreover, baseline will be used later to normalize data across all participants such that all the data can be employed in one machine learning problem to infer user intent based on data from other users. This concept is known as transfer learning.

The study presented in [28] proved that the cerebral blood velocity during right arm movement increases significantly in the contralateral MCAs than the ipsilateral MCAs while left arm movement induces bilateral activation. One of the objectives behind this paper was to confirm if the same phenomenon happens during motor imagery. To achieve this aim, we calculated the difference between left and right fTCD channels in both time and frequency domains during left and right motor imagery tasks. In time domain, we calculated the difference between average envelope signals of left and right fTCD channels during left and right motor imagery tasks as shown in Fig. 7. (a). Moreover, in frequency domain, we calculated the difference between average values of the fTCD power spectrum features, described in section 2(D), of left and right fTCD channels during left and right motor imagery tasks as seen in Fig. 7 (b). It was found that the difference between left and right channels is much higher for the right arm motor imagery with the left channel giving higher feature values while a smaller difference between the 2 channels was observed during left arm motor imagery as seen in Fig. 7 (a). This difference (CH2-CH1) during left arm motor imagery was much smaller than the difference during right arm motor imagery in the frequency ranges from 500 Hz to 750 Hz and from 1100Hz to 1800 Hz as shown in Fig. 7 (b). The reported results conform with the findings obtained using actual physical right arm movement [28] as the contralateral MCAs showed higher activation compared to the ipsilateral MCAs. In contrast, left arm motor imagery did not produce bilateral activation as expected. However, the difference in feature values between left and right fTCD channels during left arm motor imagery was smaller at specific frequency ranges.

In summary, as described above, through our time and frequency domain analyses to compare our work with [28], we showed that motor imagery induces differences in fTCD that could enable the separation among right arm MI vs left arm MI vs baseline.

Table 6 shows comparison between our method and the existing hybrid EEG-fNIRS BCIs that employ motor imagery tasks [36], [37], [38], [39], [40]. Comparisons were performed in terms of trial length and accuracy. In table 6, we included the accuracies for the three binary problems achieved using subject-specific thresholds. The proposed hybrid BCI outperformed all methods in comparison in terms of trial length since it does not require baseline/rest periods before/after each task. Therefore, we claim that the proposed hybrid BCI is faster than EEG-fNIRS BCIs and it can be used to design real-time BCI applications especially that, after the presentation of 10-s trial, the user intent can be identified within milliseconds. In terms of accuracy, we achieved similar or higher accuracies with shorter task duration. However, the system suggested by Buccino et al. [40] obtained 94.20% accuracy which is higher than the best accuracy achieved by our system, but that system is slower than ours since it requires 6 s baseline before starting each trial.

TABLE 6
Comparison between the proposed hybrid system and the state of the art hybrid EEG-fNIRS BCIs employing motor imagery tasks.

Method	BCI Type	Task Type	Accuracy	Trial length (s)	
				Task	Baseline/rest
[36] Fazli et al., 2012	EEG+fNIRS	Right/left hand gripping MI	83.20%	15	6/0
[37] Blokland et al., 2014	EEG+fNIRS	Finger & thumb tapping MI /Rest	79.00%	15	0/30±3
[38] Yin et al., 2015	EEG+fNIRS	Right hand clenching force/ speed MI	89.00%	10	0/21±1
[39] Koo et al. 2015	fTCD+NIRS	Right/left hand grasp MI	88.00%	15	0/60
[40] Buccino et al., 2016	EEG+fNIRS	Right/left arm raising & hand gripping MI	72.20%	6	6/0
[40] Buccino et al., 2016	EEG+fNIRS	Arm raising & hand gripping MI /Rest	94.20%	6	6/0
Proposed method	EEG+fTCD	Right MI/baseline	**88.33%**	10	NA
Proposed method	EEG+fTCD	Left MI/baseline	**89.48%**	10	NA
Proposed method	EEG+fTCD	Right /left MI	**82.38%**	10	NA

*NA: Not applicable

To improve the accuracy for right arm MI versus left arm MI since it is significantly lower than the accuracies obtained for right/left MI versus baseline problems, our future directions include using common spatial pattern (CSP) for EEG analysis instead of power spectrum since CSP was proved to be successful with motor imagery BCIs [36], [39], [40]. Moreover, given that the most efficient fTCD-based BCI in literature employed wavelet analysis, we plan to use wavelet decomposition for analyzing fTCD data due to MI and baseline tasks. Both the number of decomposition levels and the mother wavelet to be used will be optimized to achieve the best possible accuracy.

Recently, the ultrasound was considered as a potential brain stimulation modality. It was found that focused ultrasound energy transmitted through human brain can change EEG oscillatory dynamics. In particular, it was proved that the ultrasonic energy targeted to somatosensory cortex affect the phase of beta frequency band found in brain electrical activity [41]. However, in the current study, we are interested in proving the significance of the hybrid system compared to EEG only in terms of accuracy and information transfer rate even if such improvement occurred due to ultrasound stimulation.

V. CONCLUSION

In this paper, we propose a novel motor imagery hybrid BCI that uses EEG as the primary sensing modality that measures brain electrical activity and the fTCD as the secondary sensing modality that measures cerebral blood flow velocity. To test the feasibility of binary BCIs, 3 binary selection problems were studied including right arm MI versus baseline, left arm MI versus baseline, and

TABLE A1

Maximum accuracy (Acc) and the corresponding sensitivity (Se), specificity (Sp), and time for each subject using hybrid system, EEG only, and fTCD only. These measures were obtained for right arm MI vs baseline problem using subject-independent threshold.

Sub_ID	Time(s)	Se_Hybrid	Sp_Hybrid	Acc_Hybrid	Se_EEG	Sp_EEG	Acc_EEG	Se_fTCD	Sp_fTCD	Acc_fTCD
1	10	98.08%	88.64%	**93.75%**	96.15%	86.36%	91.67%	55.77%	59.09%	57.29%
2	10	82.69%	84.09%	83.33%	82.69%	84.09%	83.33%	67.31%	43.18%	56.26%
3	2	84.62%	84.09%	**84.38%**	80.77%	77.27%	79.17%	55.77%	34.09%	45.83%
4	9	92.31%	81.82%	**87.50%**	90.38%	70.45%	81.25%	63.46%	45.45%	55.21%
5	9	92.31%	88.64%	**90.63%**	90.38%	84.09%	87.50%	63.46%	59.09%	61.46%
6	4	82.69%	81.82%	**82.29%**	78.85%	65.91%	72.92%	61.54%	50.00%	56.25%
7	6	90.38%	75.00%	**83.33%**	80.77%	77.27%	79.17%	55.77%	56.82%	56.25%
8	7	92.31%	86.36%	**89.58%**	84.62%	75.00%	80.21%	69.23%	63.64%	66.67%
9	5	65.38%	79.55%	71.88%	78.85%	68.18%	73.96%	53.85%	70.45%	61.46%
10	10	92.31%	88.64%	**90.63%**	88.46%	84.09%	86.46%	65.38%	75.00%	69.79%
Mean	**7.2**	**87.31%**	**83.86%**	**85.73%**	85.19%	77.27%	81.56%	61.15%	55.68%	58.65%

TABLE A2

Maximum accuracy (Acc) and the corresponding sensitivity (Se), specificity (Sp), and time for each subject using hybrid system, EEG only, and fTCD only. These measures were obtained for right arm MI vs baseline problem using subject-specific thresholds.

Sub_ID	Time(s)	Se_Hybrid	Sp_Hybrid	Acc_Hybrid	Se_EEG	Sp_EEG	Acc_EEG	Se_fTCD	Sp_fTCD	Acc_fTCD
1	10	98.08%	90.91%	**94.79%**	92.31%	90.91%	91.67%	55.77%	63.64%	59.38%
2	7	96.15%	88.64%	**92.71%**	94.23%	88.64%	91.67%	88.46%	29.55%	61.46%
3	7	84.62%	88.64%	**86.46%**	78.85%	84.09%	81.25%	48.08%	54.55%	51.04%
4	9	92.31%	81.82%	**87.50%**	90.38%	70.45%	81.25%	63.46%	45.45%	55.21%
5	9	92.31%	88.64%	**90.63%**	90.38%	84.09%	87.50%	63.46%	59.09%	61.46%
6	7	88.64%	84.09%	**86.46%**	86.54%	84.09%	85.42%	67.31%	43.18%	56.25%
7	6	92.31%	79.55%	**86.46%**	84.62%	75.00%	80.21%	46.15%	50.00%	47.92%
8	7	96.15%	86.36%	**91.67%**	84.62%	77.27%	81.25%	73.08%	65.91%	69.79%
9	5	76.92%	75.00%	**76.04%**	78.85%	63.64%	71.88%	48.08%	52.27%	50.00%
10	10	92.31%	88.64%	**90.63%**	88.46%	84.09%	86.46%	65.38%	75.00%	69.79%
Mean	**7.7**	**90.96%**	**85.23%**	**88.33%**	86.92%	80.23%	83.85%	61.92%	53.86%	58.23%

right arm MI versus left arm MI. It was shown that right/left arm MI versus baseline achieved higher accuracies compared to right arm MI versus left arm MI. Specifically, right arm MI versus baseline obtained 88.33% average accuracy and left arm MI versus baseline achieved 89.48% average accuracy while right arm MI vs left arm MI got average accuracy of 82.38%. However, right arm MI versus left arm MI obtained the highest bit rate of 10.57 bits/min compared to 4.17 bits/min, and 5.45 bits/min obtained by right arm MI versus baseline and left arm MI versus baseline. Based on these results, we believe that the proposed hybrid BCI is a promising tool for developing real-time BCI applications.

APPENDIX

In Tables A1-A6, we introduce the detailed performance measures of each individual including maximum accuracy and the corresponding sensitivity, specificity, and time for the 3 classification problems solved using both subject-independent and subject-specific thresholds.

TABLE A3
Maximum accuracy (Acc) and the corresponding sensitivity (Se), specificity (Sp), and time for each subject using hybrid system, EEG only, and fTCD only. These measures were obtained for left arm MI vs baseline problem using subject-independent threshold.

Sub_ID	Time(s)	Se_Hybrid	Sp_Hybrid	Acc_Hybrid	Se _EEG	Sp _EEG	Acc_EEG	Se_fTCD	Sp_fTCD	Acc_fTCD
1	10	92.45%	95.45%	**93.81%**	86.79%	90.91%	88.66%	77.36%	70.45%	74.23%
2	7	94.34%	90.91%	92.78%	96.23%	90.91%	93.81%	77.36%	36.36%	58.76%
3	8	86.79%	93.18%	**89.69%**	81.13%	79.55%	80.41%	39.62%	54.55%	46.39%
4	2	73.58%	75.00%	**74.23%**	75.47%	70.45%	73.32%	58.49%	40.91%	50.52%
5	8	83.02%	77.27%	**80.41%**	79.25%	75.00%	77.32%	30.19%	59.09%	43.30%
6	2	92.45%	79.55%	**86.60%**	92.45%	77.27%	85.57%	64.15%	38.64%	52.58%
7	3	90.57%	90.91%	**90.72%**	88.68%	88.64%	88.66%	58.49%	50.00%	54.64%
8	9	90.57%	86.36%	**88.66%**	88.68%	84.09%	86.60%	49.06%	63.64%	55.67%
9	5	83.02%	75.00%	**79.38%**	75.47%	72.73%	74.23%	56.60%	38.64%	48.45%
10	9	88.68%	88.64%	**88.66%**	86.79%	88.64%	87.63%	52.83%	59.09%	55.67%
Mean	**6.3**	**87.55%**	**85.23**	**86.49%**	85.09%	81.82%	83.61%	56.42%	51.14%	54.02%

TABLE A4
Maximum accuracy (Acc) and the corresponding sensitivity (Se), specificity (Sp), and time for each subject using hybrid system, EEG only, and fTCD only. These measures were obtained for left arm MI vs baseline problem using subject-specific thresholds.

Sub_ID	Time(s)	Se_Hybrid	Sp_Hybrid	Acc_Hybrid	Se _EEG	Sp _EEG	Acc_EEG	Se_fTCD	Sp_fTCD	Acc_fTCD
1	10	100.00%	95.45%	**97.94%**	88.68%	86.36%	87.63%	64.15%	68.18%	65.98%
2	7	96.23%	90.91%	**93.81%**	92.45%	90.91%	91.75%	92.45%	34.09%	65.98%
3	4	94.34%	93.18%	**93.81%**	86.79%	75.00%	81.44%	43.40%	61.36%	51.55%
4	5	86.79%	75.00%	**81.44%**	84.91%	70.45%	78.35%	69.81%	52.27%	61.86%
5	9	86.79%	88.64%	87.63%	84.91%	90.91%	87.63%	58.49%	47.73%	53.61%
6	3	88.68%	84.09%	**86.60%**	75.47%	72.73%	74.23%	56.60%	50.00%	53.61%
7	3	90.57%	90.91%	**90.72%**	88.68%	88.64%	88.66%	58.49%	50.00%	54.64%
8	9	96.23%	88.64%	**92.78%**	92.45%	77.27%	85.57%	56.60%	43.18%	50.52%
9	5	83.02%	75.00%	**79.38%**	75.47%	72.73%	74.23%	56.60%	38.64%	48.45%
10	6	96.23%	84.09%	**90.72%**	94.34%	88.64%	91.75%	45.28%	50.00%	47.42%
Mean	**6.1**	**91.89%**	**86.59%**	**89.48%**	86.42%	81.36%	84.12%	60.19%	49.55%	55.36%

TABLE A5
Maximum accuracy (Acc) and the corresponding right arm and left arm sensitivities (SeR, and SeL), and time for each subject using hybrid system, EEG only, and fTCD only. These measures were obtained for right arm MI vs left arm MI problem using subject-independent threshold.

Sub_ID	Time(s)	SeR_Hybrid	SeL_Hybrid	Acc_Hybrid	SeR _EEG	SeL _EEG	Acc_EEG	SeR_fTCD	SeL_fTCD	Acc_fTCD
1	1	88.46%	84.91%	86.67%	88.46%	84.91%	86.67%	40.38%	49.06%	44.76%
2	5	73.08%	77.36%	75.24%	75.00%	75.47%	75.24%	50.00%	26.42%	38.10%
3	10	78.85%	71.70%	**75.24%**	76.92%	69.81%	73.33%	59.62%	33.96%	46.67%
4	1	86.54%	81.13%	**83.81%**	82.69%	83.02%	82.86%	59.62%	32.08%	45.71%
5	1	78.85%	84.91%	**81.90%**	76.92%	79.25%	78.10%	34.62%	66.04%	50.48%
6	3	82.69%	84.91%	83.81%	84.62%	86.79%	85.71%	46.15%	39.62%	42.86%
7	4	71.15%	71.70%	71.43%	73.08%	77.36%	75.24%	46.15%	43.40%	44.76%
8	7	94.23%	90.57%	**92.38%**	88.46%	90.57%	89.52%	51.92%	39.62%	45.71%
9	1	71.15%	71.70%	**71.43%**	76.92%	64.15%	70.48%	44.23%	45.28%	44.76%
10	1	65.38%	71.70%	**68.57%**	57.69%	73.58%	65.71%	73.08%	52.83%	62.86%
Mean	**3.4**	**79.04%**	**79.06%**	**79.05%**	78.08%	78.49%	78.29%	50.58%	42.83%	46.67%

TABLE A6

Maximum accuracy (Acc) and the corresponding right arm and left arm sensitivities (SeR, and SeL), and time for each subject using hybrid system, EEG only, and fTCD only. These measures were obtained for right arm MI vs left arm MI problem using subject-specific thresholds.

Sub_ID	Time(s)	SeR_Hybrid	SeL_Hybrid	Acc_Hybrid	SeR_EEG	SeL_EEG	Acc_EEG	SeR_fTCD	SeL_fTCD	Acc_fTCD
1	1	94.23%	92.45%	**93.33%**	82.69%	83.02%	82.86%	55.77%	47.17%	51.43%
2	5	73.08%	77.36%	75.24%	75.00%	75.47%	75.24%	50.00%	26.42%	38.10%
3	6	78.85%	84.91%	**81.90%**	71.15%	71.70%	71.43%	67.31%	71.70%	69.52%
4	2	86.54%	84.91%	**85.71%**	84.62%	79.25%	81.90%	63.46%	43.40%	53.33%
5	1	78.85%	84.91%	**81.90%**	76.92%	79.25%	78.10%	34.62%	66.04%	50.48%
6	3	82.69%	84.91%	83.81%	84.62%	86.79%	85.71%	46.15%	39.62%	42.86%
7	4	84.62%	73.58%	**79.05%**	71.15%	71.70%	71.43%	36.54%	50.94%	43.81%
8	9	98.08%	96.23%	**97.14%**	98.08%	94.34%	96.19%	50.00%	50.00%	50.00%
9	1	71.15%	71.70%	**71.43%**	76.92%	64.15%	70.48%	44.23%	45.28%	44.76%
10	2	73.08%	75.47%	**74.29%**	65.38%	60.38%	62.86%	76.92%	56.60%	66.67%
Mean	**3.4**	**82.12%**	**82.64%**	**82.38%**	78.65%	76.60%	77.62%	52.50%	49.72%	51.10%

REFERENCES

[1] T. S. Davis, H. A. C. Wark, D. T. Hutchinson, D. J. Warren, K. O'Neill, T. Scheinblum, G. A. Clark, R. A. Normann, and B. Greger, "Restoring motor control and sensory feedback in people with upper extremity amputations using arrays of 96 microelectrodes implanted in the median and ulnar nerves," *J. Neural Eng.*, vol. 13, no. 3, p. 036001, Jun. 2016.

[2] R. Zhang, Y. Li, Y. Yan, H. Zhang, S. Wu, T. Yu, and Z. Gu, "Control of a Wheelchair in an Indoor Environment Based on a Brain-Computer Interface and Automated Navigation," *IEEE Trans. Neural Syst. Rehabil. Eng.*, vol. 24, no. 1, pp. 128–139, Jan. 2016.

[3] L. F. Nicolas-Alonso and J. Gomez-Gil, "Brain computer interfaces, a review.," *Sensors (Basel).*, vol. 12, no. 2, pp. 1211–79, 2012.

[4] S. Qiu, Z. Li, W. He, L. Zhang, C. Yang, and C.-Y. Su, "Brain–Machine Interface and Visual Compressive Sensing-Based Teleoperation Control of an Exoskeleton Robot," *IEEE Trans. Fuzzy Syst.*, vol. 25, no. 1, pp. 58–69, Feb. 2017.

[5] M. Kryger, B. Wester, E. A. Pohlmeyer, M. Rich, B. John, J. Beaty, M. McLoughlin, M. Boninger, and E. C. Tyler-Kabara, "Flight simulation using a Brain-Computer Interface: A pilot, pilot study," *Exp. Neurol.*, vol. 287, pp. 473–478, Jan. 2017.

[6] J. Faller, B. Z. Allison, C. Brunner, R. Scherer, D. Schmalstieg, G. Pfurtscheller, and C. Neuper, "A feasibility study on SSVEP-based interaction with motivating and immersive virtual and augmented reality," Jan. 2017.

[7] N. Naseer and K.-S. Hong, "fNIRS-based brain-computer interfaces: a review," *Front. Hum. Neurosci.*, vol. 9, p. 3, Jan. 2015.

[8] M. O. Sokunbi, D. E. J. Linden, I. Habes, S. Johnston, and N. Ihssen, "Real-time fMRI brain-computer interface: development of a â€œmotivational feedbackâ€• subsystem for the regulation of visual cue reactivity," *Front. Behav. Neurosci.*, vol. 8, p. 392, Nov. 2014.

[9] T. N. Lal, N. Birbaumer, B. Schölkopf, M. Schröder, N. J. Hill, H. Preissl, T. Hinterberger, J. Mellinger, M. Bogdan, W. Rosenstiel, and T. Hofmann, "A brain computer interface with online feedback based on magnetoencephalography," in *Proceedings of the 22nd international conference on Machine learning - ICML '05*, 2005, pp. 465–472.

[10] B. Z. Allison, E. W. Wolpaw, and J. R. Wolpaw, "Brain-computer interface systems: progress and prospects.," *Expert Rev. Med. Devices*, vol. 4, no. 4, pp. 463–74, Jul. 2007.

[11] P. V. Zephaniah and J. G. Kim, "Recent functional near infrared spectroscopy based brain computer interface systems: Developments, applications and challenges," *Biomed. Eng. Lett.*, vol. 4, no. 3, pp. 223–230, Sep. 2014.

[12] L. E. H. van Dokkum, T. Ward, and I. Laffont, "Brain computer interfaces for neurorehabilitation – its current status as a rehabilitation strategy post-stroke," *Ann. Phys. Rehabil. Med.*, vol. 58, no. 1, pp. 3–8, Feb. 2015.

[13] A. Schlögl, F. Lee, H. Bischof, and G. Pfurtscheller, "Characterization of four-class motor imagery EEG data for the BCI-competition 2005," *J. Neural Eng.*, vol. 2, no. 4, pp. L14–L22, Dec. 2005.

[14] K. K. Kai Keng Ang, C. Cuntai Guan, K. S. G. Chua, B. T. Beng Ti Ang, C. Kuah, C. Chuanchu Wang, K. S. Kok Soon Phua, Z. Y. Zheng Yang Chin, and H. Haihong Zhang, "Clinical study of neurorehabilitation in stroke using EEG-based motor imagery brain-computer interface with robotic feedback," in *2010 Annual International Conference of the IEEE Engineering in Medicine and Biology*, 2010, vol. 2010, pp. 5549–5552.

[15] K. K. Ang and C. Guan, "EEG-Based Strategies to Detect Motor Imagery for Control and Rehabilitation," *IEEE Trans. Neural Syst. Rehabil. Eng.*, vol. 25, no. 4, pp. 392–401, Apr. 2017.

[16] K. LaFleur, K. Cassady, A. Doud, K. Shades, E. Rogin, and B. He, "Quadcopter control in three-dimensional space using a noninvasive motor imagery-based brain–computer interface," *J. Neural Eng.*, vol. 10, no. 4, p. 046003, Aug. 2013.

[17] A. A. Blank, J. A. French, A. U. Pehlivan, and M. K. O'Malley, "Current Trends in Robot-Assisted Upper-Limb Stroke Rehabilitation: Promoting Patient Engagement in Therapy," *Curr. Phys. Med. Rehabil. Reports*, vol. 2, no. 3, pp. 184–195, Sep. 2014.

[18] S. Fazli, S. Dahne, W. Samek, F. Bieszmann, and K.-R. Muller, "Learning From More Than One Data Source: Data Fusion Techniques for Sensorimotor Rhythm-Based Brain&#x2013;Computer Interfaces," *Proc. IEEE*, vol. 103, no. 6, pp. 891–906, Jun. 2015.

[19] G. Muller-Putz, R. Leeb, M. Tangermann, J. Hohne, A. Kubler, F. Cincotti, D. Mattia, R. Rupp, K.-R. Muller, and J. del R. Millan, "Towards Noninvasive

Hybrid Brain-Computer Interfaces: Framework, Practice, Clinical Application, and Beyond," *Proc. IEEE*, vol. 103, no. 6, pp. 926–943, Jun. 2015.

[20] H. Morioka, A. Kanemura, S. Morimoto, T. Yoshioka, S. Oba, M. Kawanabe, and S. Ishii, "Decoding spatial attention by using cortical currents estimated from electroencephalography with near-infrared spectroscopy prior information," *Neuroimage*, vol. 90, pp. 128–139, Apr. 2014.

[21] B.-K. Min, M. J. Marzelli, and S.-S. Yoo, "Neuroimaging-based approaches in the brain–computer interface," *Trends Biotechnol.*, vol. 28, no. 11, pp. 552–560, Nov. 2010.

[22] A. Khalaf, M. Sybeldon, E. Sejdic, and M. Akcakaya, "A brain-computer interface based on functional transcranial doppler ultrasound using wavelet transform and support vector machines," *J. Neurosci. Methods*, vol. 293, 2018.

[23] A. V. Alexandrov, M. A. Sloan, L. K. S. Wong, C. Douville, A. Y. Razumovsky, W. J. Koroshetz, M. Kaps, and C. H. Tegeler, "Practice Standards for Transcranial Doppler Ultrasound: Part I-Test Performance," *J. Neuroimaging*, vol. 17, no. 1, pp. 11–18, Jan. 2007.

[24] A. J. B. Myrden, A. Kushki, E. Sejdić, A.-M. Guerguerian, and T. Chau, "A Brain-Computer Interface Based on Bilateral Transcranial Doppler Ultrasound," *PLoS One*, vol. 6, no. 9, p. e24170, Sep. 2011.

[25] I. Aleem and T. Chau, "Towards a hemodynamic BCI using transcranial Doppler without user-specific training data," *J. Neural Eng.*, vol. 10, no. 1, p. 016005, Feb. 2013.

[26] J. Lu, K. A. Mamun, and T. Chau, "Pattern classification to optimize the performance of Transcranial Doppler Ultrasonography-based brain machine interface," 2015.

[27] A. Khalaf, M. Sybeldon, E. Sejdic, and M. Akcakaya, "A brain-computer interface based on functional transcranial doppler ultrasound using wavelet transform and support vector machines," *J. Neurosci. Methods*, vol. 293, pp. 174–182, Jan. 2018.

[28] M. Matteis, F. Federico, E. Troisi, P. Pasqualetti, F. Vernieri, C. Caltagirone, L. Petrosini, and M. Silvestrini, "Cerebral blood flow velocity changes during meaningful and meaningless gestures - a functional transcranial Doppler study," *Eur. J. Neurol.*, vol. 13, no. 1, pp. 24–29, Jan. 2006.

[29] N. Stroobant and G. Vingerhoets, "Transcranial Doppler ultrasonography monitoring of cerebral hemodynamics during performance of cognitive tasks: a review.," *Neuropsychol. Rev.*, vol. 10, no. 4, pp. 213–31, Dec. 2000.

[30] L. H. Monsein, A. Y. Razumovsky, S. J. Ackerman, H. J. W. Nauta, and D. F. Hanley, "Validation of transcranial Doppler ultrasound with a stereotactic neurosurgical technique," *J. Neurosurg.*, vol. 82, no. 6, pp. 972–975, Jun. 1995.

[31] P. D. Welch and P. D., "The Use of Fast Fourier Transform for the Estimation of Power Spectra: A Method Based on Time Averaging Over Short, Modified Periodograms," *IEEE Trans. Audio Electroacoust., Vol. AU-15, p. 70-73*, vol. 15, pp. 70–73, 1967.

[32] Hanchuan Peng, Fuhui Long, and C. Ding, "Feature selection based on mutual information criteria of max-dependency, max-relevance, and min-redundancy," *IEEE Trans. Pattern Anal. Mach. Intell.*, vol. 27, no. 8, pp. 1226–1238, Aug. 2005.

[33] J. R. Vergara and P. A. Estévez, "A review of feature selection methods based on mutual information," *Neural Comput. Appl.*, vol. 24, no. 1, pp. 175–186, Jan. 2014.

[34] C.-W. Chih-Wei Hsu and C.-J. Chih-Jen Lin, "A comparison of methods for multiclass support vector machines," *IEEE Trans. Neural Networks*, vol. 13, no. 2, pp. 415–425, Mar. 2002.

[35] R. C. Blair and J. J. Higgins, "A Comparison of the Power of Wilcoxon's Rank-Sum Statistic to That of Student's t Statistic under Various Nonnormal Distributions," *J. Educ. Stat.*, vol. 5, no. 4, p. 309, 1980.

[36] S. Fazli, J. Mehnert, J. Steinbrink, G. Curio, A. Villringer, K.-R. Müller, and B. Blankertz, "Enhanced performance by a hybrid NIRS–EEG brain computer interface," *Neuroimage*, vol. 59, no. 1, pp. 519–529, Jan. 2012.

[37] Y. Blokland, L. Spyrou, D. Thijssen, T. Eijsvogels, W. Colier, M. Floor-Westerdijk, R. Vlek, J. Bruhn, and J. Farquhar, "Combined EEG-fNIRS Decoding of Motor Attempt and Imagery for Brain Switch Control: An Offline Study in Patients With Tetraplegia," *IEEE Trans. Neural Syst. Rehabil. Eng.*, vol. 22, no. 2, pp. 222–229, Mar. 2014.

[38] X. Yin, B. Xu, C. Jiang, Y. Fu, Z. Wang, H. Li, and G. Shi, "A hybrid BCI based on EEG and fNIRS signals improves the performance of decoding motor imagery of both force and speed of hand clenching," *J. Neural Eng.*, vol. 12, no. 3, p. 036004, Jun. 2015.

[39] B. Koo, H.-G. Lee, Y. Nam, H. Kang, C. S. Koh, H.-C. Shin, and S. Choi, "A hybrid NIRS-EEG system for self-paced brain computer interface with online motor imagery," *J. Neurosci. Methods*, vol. 244, pp. 26–32, Apr. 2015.

[40] A. P. Buccino, H. O. Keles, and A. Omurtag, "Hybrid EEG-fNIRS Asynchronous Brain-Computer Interface for Multiple Motor Tasks," *PLoS One*, vol. 11, no. 1, p. e0146610, Jan. 2016.

[41] J. Mueller, W. Legon, A. Opitz, T. F. Sato, and W. J. Tyler, "Transcranial Focused Ultrasound Modulates Intrinsic and Evoked EEG Dynamics," Brain Stimul., vol. 7, no. 6, pp. 900–908, Nov. 2014.
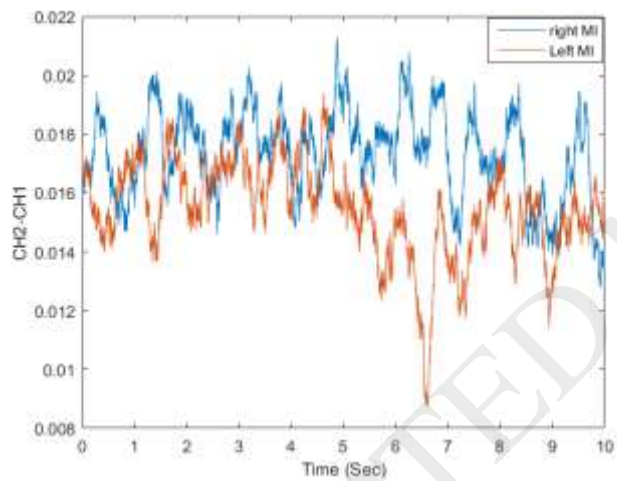
Fig. 7. Difference between left fTCD channel (channel 2) and right fTCD channel (channel 1) during right arm and left arm MI for a) fTCD normalized envelope signals in time domain   b) power spectrum features in frequency domain.